EUROPEAN ORGANIZATION FOR NUCLEAR RESEARCH (CERN)

CERN-PH-EP-2014-016
LHCb-PAPER-2013-066
25 March 2014

arXiv:1402.2539v2 [hep-ex] 24 Apr 2014

Measurement of Υ production in pp collisions at $\sqrt{s} = 2.76$ TeV

The LHCb collaboration*

Abstract

The production of $\Upsilon(1S)$, $\Upsilon(2S)$ and $\Upsilon(3S)$ mesons decaying into the dimuon final state is studied with the LHCb detector using a data sample corresponding to an integrated luminosity of $3.3\,\text{pb}^{-1}$ collected in proton-proton collisions at a centre-of-mass energy of $\sqrt{s} = 2.76$ TeV. The differential production cross-sections times dimuon branching fractions are measured as functions of the Υ transverse momentum and rapidity, over the ranges $p_{\rm T} < 15$ GeV/c and $2.0 < y < 4.5$. The total cross-sections in this kinematic region, assuming unpolarised production, are measured to be

$$\begin{aligned}
\sigma\left(\text{pp} \to \Upsilon(1S)\text{X}\right) \times \mathcal{B}\left(\Upsilon(1S) \to \mu^+\mu^-\right) &= 1.111 \pm 0.043 \pm 0.044\,\text{nb}, \\
\sigma\left(\text{pp} \to \Upsilon(2S)\text{X}\right) \times \mathcal{B}\left(\Upsilon(2S) \to \mu^+\mu^-\right) &= 0.264 \pm 0.023 \pm 0.011\,\text{nb}, \\
\sigma\left(\text{pp} \to \Upsilon(3S)\text{X}\right) \times \mathcal{B}\left(\Upsilon(3S) \to \mu^+\mu^-\right) &= 0.159 \pm 0.020 \pm 0.007\,\text{nb},
\end{aligned}$$

where the first uncertainty is statistical and the second systematic.

Submitted to Eur. Phys. J. C

© CERN on behalf of the LHCb collaboration, license CC-BY-3.0.

*Authors are listed on the following pages.

LHCb collaboration

R. Aaij[41], B. Adeva[37], M. Adinolfi[46], A. Affolder[52], Z. Ajaltouni[5], J. Albrecht[9], F. Alessio[38], M. Alexander[51], S. Ali[41], G. Alkhazov[30], P. Alvarez Cartelle[37], A.A. Alves Jr[25], S. Amato[2], S. Amerio[22], Y. Amhis[7], L. Anderlini[17,g], J. Anderson[40], R. Andreassen[57], M. Andreotti[16,f], J.E. Andrews[58], R.B. Appleby[54], O. Aquines Gutierrez[10], F. Archilli[38], A. Artamonov[35], M. Artuso[59], E. Aslanides[6], G. Auriemma[25,n], M. Baalouch[5], S. Bachmann[11], J.J. Back[48], A. Badalov[36], V. Balagura[31], W. Baldini[16], R.J. Barlow[54], C. Barschel[39], S. Barsuk[7], W. Barter[47], V. Batozskaya[28], Th. Bauer[41], A. Bay[39], J. Beddow[51], F. Bedeschi[23], I. Bediaga[1], S. Belogurov[31], K. Belous[35], I. Belyaev[31], E. Ben-Haim[8], G. Bencivenni[18], S. Benson[50], J. Benton[46], A. Berezhnoy[32], R. Bernet[40], M.-O. Bettler[47], M. van Beuzekom[41], A. Bien[11], S. Bifani[45], T. Bird[54], A. Bizzeti[17,i], P.M. Bjørnstad[54], T. Blake[48], F. Blanc[39], J. Blouw[10], S. Blusk[59], V. Bocci[25], A. Bondar[34], N. Bondar[30], W. Bonivento[15,38], S. Borghi[54], A. Borgia[59], M. Borsato[7], T.J.V. Bowcock[52], E. Bowen[40], C. Bozzi[16], T. Brambach[9], J. van den Brand[42], J. Bressieux[39], D. Brett[54], M. Britsch[10], T. Britton[59], N.H. Brook[46], H. Brown[52], A. Bursche[40], G. Busetto[22,r], J. Buytaert[38], S. Cadeddu[15], R. Calabrese[16,f], O. Callot[7], M. Calvi[20,k], M. Calvo Gomez[36,p], A. Camboni[36], P. Campana[18,38], D. Campora Perez[38], A. Carbone[14,d], G. Carboni[24,l], R. Cardinale[19,j], A. Cardini[15], H. Carranza-Mejia[50], L. Carson[50], K. Carvalho Akiba[2], G. Casse[52], L. Castillo Garcia[38], M. Cattaneo[38], Ch. Cauet[9], R. Cenci[58], M. Charles[8], Ph. Charpentier[38], S.-F. Cheung[55], N. Chiapolini[40], M. Chrzaszcz[40,26], K. Ciba[38], X. Cid Vidal[38], G. Ciezarek[53], P.E.L. Clarke[50], M. Clemencic[38], H.V. Cliff[47], J. Closier[38], C. Coca[29], V. Coco[38], J. Cogan[6], E. Cogneras[5], P. Collins[38], A. Comerma-Montells[36], A. Contu[15,38], A. Cook[46], M. Coombes[46], S. Coquereau[8], G. Corti[38], I. Counts[56], B. Couturier[38], G.A. Cowan[50], D.C. Craik[48], M. Cruz Torres[60], S. Cunliffe[53], R. Currie[50], C. D'Ambrosio[38], J. Dalseno[46], P. David[8], P.N.Y. David[41], A. Davis[57], I. De Bonis[4], K. De Bruyn[41], S. De Capua[54], M. De Cian[11], J.M. De Miranda[1], L. De Paula[2], W. De Silva[57], P. De Simone[18], D. Decamp[4], M. Deckenhoff[9], L. Del Buono[8], N. Déléage[4], D. Derkach[55], O. Deschamps[5], F. Dettori[42], A. Di Canto[11], H. Dijkstra[38], S. Donleavy[52], F. Dordei[11], M. Dorigo[39], P. Dorosz[26,o], A. Dosil Suárez[37], D. Dossett[48], A. Dovbnya[43], F. Dupertuis[39], P. Durante[38], R. Dzhelyadin[35], A. Dziurda[26], A. Dzyuba[30], S. Easo[49], U. Egede[53], V. Egorychev[31], S. Eidelman[34], S. Eisenhardt[50], U. Eitschberger[9], R. Ekelhof[9], L. Eklund[51,38], I. El Rifai[5], Ch. Elsasser[40], S. Esen[11], A. Falabella[16,f], C. Färber[11], C. Farinelli[41], S. Farry[52], D. Ferguson[50], V. Fernandez Albor[37], F. Ferreira Rodrigues[1], M. Ferro-Luzzi[38], S. Filippov[33], M. Fiore[16,f], M. Fiorini[16,f], C. Fitzpatrick[38], M. Fontana[10], F. Fontanelli[19,j], R. Forty[38], O. Francisco[2], M. Frank[38], C. Frei[38], M. Frosini[17,38,g], J. Fu[21], E. Furfaro[24,l], A. Gallas Torreira[37], D. Galli[14,d], M. Gandelman[2], P. Gandini[59], Y. Gao[3], J. Garofoli[59], J. Garra Tico[47], L. Garrido[36], C. Gaspar[38], R. Gauld[55], E. Gersabeck[11], M. Gersabeck[54], T. Gershon[48], Ph. Ghez[4], A. Gianelle[22], S. Giani'[39], V. Gibson[47], L. Giubega[29], V.V. Gligorov[38], C. Göbel[60], D. Golubkov[31], A. Golutvin[53,31,38], A. Gomes[1,a], H. Gordon[38], M. Grabalosa Gándara[5], R. Graciani Diaz[36], L.A. Granado Cardoso[38], E. Graugés[36], G. Graziani[17], A. Grecu[29], E. Greening[55], S. Gregson[47], P. Griffith[45], L. Grillo[11], O. Grünberg[61], B. Gui[59], E. Gushchin[33], Yu. Guz[35,38], T. Gys[38], C. Hadjivasiliou[59], G. Haefeli[39], C. Haen[38], T.W. Hafkenscheid[64], S.C. Haines[47], S. Hall[53], B. Hamilton[58], T. Hampson[46], S. Hansmann-Menzemer[11], N. Harnew[55], S.T. Harnew[46], J. Harrison[54], T. Hartmann[61], J. He[38], T. Head[38], V. Heijne[41], K. Hennessy[52], P. Henrard[5], L. Henry[8], J.A. Hernando Morata[37], E. van Herwijnen[38], M. Heß[61], A. Hicheur[1], D. Hill[55], M. Hoballah[5], C. Hombach[54],

W. Hulsbergen[41], P. Hunt[55], N. Hussain[55], D. Hutchcroft[52], D. Hynds[51], V. Iakovenko[44], M. Idzik[27], P. Ilten[56], R. Jacobsson[38], A. Jaeger[11], E. Jans[41], P. Jaton[39], A. Jawahery[58], F. Jing[3], M. John[55], D. Johnson[55], C.R. Jones[47], C. Joram[38], B. Jost[38], N. Jurik[59], M. Kaballo[9], S. Kandybei[43], W. Kanso[6], M. Karacson[38], T.M. Karbach[38], M. Kelsey[59], I.R. Kenyon[45], T. Ketel[42], B. Khanji[20], C. Khurewathanakul[39], S. Klaver[54], O. Kochebina[7], I. Komarov[39], R.F. Koopman[42], P. Koppenburg[41], M. Korolev[32], A. Kozlinskiy[41], L. Kravchuk[33], K. Kreplin[11], M. Kreps[48], G. Krocker[11], P. Krokovny[34], F. Kruse[9], M. Kucharczyk[20,26,38,k], V. Kudryavtsev[34], K. Kurek[28], T. Kvaratskheliya[31,38], V.N. La Thi[39], D. Lacarrere[38], G. Lafferty[54], A. Lai[15], D. Lambert[50], R.W. Lambert[42], E. Lanciotti[38], G. Lanfranchi[18], C. Langenbruch[38], T. Latham[48], C. Lazzeroni[45], R. Le Gac[6], J. van Leerdam[41], J.-P. Lees[4], R. Lefèvre[5], A. Leflat[32], J. Lefrançois[7], S. Leo[23], O. Leroy[6], T. Lesiak[26], B. Leverington[11], Y. Li[3], M. Liles[52], R. Lindner[38], C. Linn[11], F. Lionetto[40], B. Liu[15], G. Liu[38], S. Lohn[38], I. Longstaff[51], J.H. Lopes[2], N. Lopez-March[39], P. Lowdon[40], H. Lu[3], D. Lucchesi[22,r], J. Luisier[39], H. Luo[50], E. Luppi[16,f], O. Lupton[55], F. Machefert[7], I.V. Machikhiliyan[31], F. Maciuc[29], O. Maev[30,38], S. Malde[55], G. Manca[15,e], G. Mancinelli[6], M. Manzali[16,f], J. Maratas[5], U. Marconi[14], P. Marino[23,t], R. Märki[39], J. Marks[11], G. Martellotti[25], A. Martens[8], A. Martín Sánchez[7], M. Martinelli[41], D. Martinez Santos[42], F. Martinez Vidal[63], D. Martins Tostes[2], A. Massafferri[1], R. Matev[38], Z. Mathe[38], C. Matteuzzi[20], A. Mazurov[16,38,f], M. McCann[53], J. McCarthy[45], A. McNab[54], R. McNulty[12], B. McSkelly[52], B. Meadows[57,55], F. Meier[9], M. Meissner[11], M. Merk[41], D.A. Milanes[8], M.-N. Minard[4], J. Molina Rodriguez[60], S. Monteil[5], D. Moran[54], M. Morandin[22], P. Morawski[26], A. Mordà[6], M.J. Morello[23,t], R. Mountain[59], F. Muheim[50], K. Müller[40], R. Muresan[29], B. Muryn[27], B. Muster[39], P. Naik[46], T. Nakada[39], R. Nandakumar[49], I. Nasteva[1], M. Needham[50], N. Neri[21], S. Neubert[38], N. Neufeld[38], A.D. Nguyen[39], T.D. Nguyen[39], C. Nguyen-Mau[39,q], M. Nicol[7], V. Niess[5], R. Niet[9], N. Nikitin[32], T. Nikodem[11], A. Novoselov[35], A. Oblakowska-Mucha[27], V. Obraztsov[35], S. Oggero[41], S. Ogilvy[51], O. Okhrimenko[44], R. Oldeman[15,e], G. Onderwater[64], M. Orlandea[29], J.M. Otalora Goicochea[2], P. Owen[53], A. Oyanguren[36], B.K. Pal[59], A. Palano[13,c], F. Palombo[21,u], M. Palutan[18], J. Panman[38], A. Papanestis[49,38], M. Pappagallo[51], L. Pappalardo[16], C. Parkes[54], C.J. Parkinson[9], G. Passaleva[17], G.D. Patel[52], M. Patel[53], C. Patrignani[19,j], C. Pavel-Nicorescu[29], A. Pazos Alvarez[37], A. Pearce[54], A. Pellegrino[41], G. Penso[25,m], M. Pepe Altarelli[38], S. Perazzini[14,d], E. Perez Trigo[37], P. Perret[5], M. Perrin-Terrin[6], L. Pescatore[45], E. Pesen[65], G. Pessina[20], K. Petridis[53], A. Petrolini[19,j], E. Picatoste Olloqui[36], B. Pietrzyk[4], T. Pilař[48], D. Pinci[25], A. Pistone[19], S. Playfer[50], M. Plo Casasus[37], F. Polci[8], G. Polok[26], A. Poluektov[48,34], E. Polycarpo[2], A. Popov[35], D. Popov[10], B. Popovici[29], C. Potterat[36], A. Powell[55], J. Prisciandaro[39], A. Pritchard[52], C. Prouve[46], V. Pugatch[44], A. Puig Navarro[39], G. Punzi[23,s], W. Qian[4], B. Rachwal[26], J.H. Rademacker[46], B. Rakotomiaramanana[39], M. Rama[18], M.S. Rangel[2], I. Raniuk[43], N. Rauschmayr[38], G. Raven[42], S. Redford[55], S. Reichert[54], M.M. Reid[48], A.C. dos Reis[1], S. Ricciardi[49], A. Richards[53], K. Rinnert[52], V. Rives Molina[36], D.A. Roa Romero[5], P. Robbe[7], D.A. Roberts[58], A.B. Rodrigues[1], E. Rodrigues[54], P. Rodriguez Perez[37], S. Roiser[38], V. Romanovsky[35], A. Romero Vidal[37], M. Rotondo[22], J. Rouvinet[39], T. Ruf[38], F. Ruffini[23], H. Ruiz[36], P. Ruiz Valls[36], G. Sabatino[25,l], J.J. Saborido Silva[37], N. Sagidova[30], P. Sail[51], B. Saitta[15,e], V. Salustino Guimaraes[2], B. Sanmartin Sedes[37], R. Santacesaria[25], C. Santamarina Rios[37], E. Santovetti[24,l], M. Sapunov[6], A. Sarti[18], C. Satriano[25,n], A. Satta[24], M. Savrie[16,f], D. Savrina[31,32], M. Schiller[42], H. Schindler[38], M. Schlupp[9], M. Schmelling[10], B. Schmidt[38], O. Schneider[39], A. Schopper[38], M.-H. Schune[7], R. Schwemmer[38], B. Sciascia[18], A. Sciubba[25], M. Seco[37], A. Semennikov[31],

K. Senderowska[27], I. Sepp[53], N. Serra[40], J. Serrano[6], P. Seyfert[11], M. Shapkin[35], I. Shapoval[16,43,f], Y. Shcheglov[30], T. Shears[52], L. Shekhtman[34], O. Shevchenko[43], V. Shevchenko[62], A. Shires[9], R. Silva Coutinho[48], G. Simi[22], M. Sirendi[47], N. Skidmore[46], T. Skwarnicki[59], N.A. Smith[52], E. Smith[55,49], E. Smith[53], J. Smith[47], M. Smith[54], H. Snoek[41], M.D. Sokoloff[57], F.J.P. Soler[51], F. Soomro[39], D. Souza[46], B. Souza De Paula[2], B. Spaan[9], A. Sparkes[50], F. Spinella[23], P. Spradlin[51], F. Stagni[38], S. Stahl[11], O. Steinkamp[40], S. Stevenson[55], S. Stoica[29], S. Stone[59], B. Storaci[40], S. Stracka[23,38], M. Straticiuc[29], U. Straumann[40], R. Stroili[22], V.K. Subbiah[38], L. Sun[57], W. Sutcliffe[53], S. Swientek[9], V. Syropoulos[42], M. Szczekowski[28], P. Szczypka[39,38], D. Szilard[2], T. Szumlak[27], S. T'Jampens[4], M. Teklishyn[7], G. Tellarini[16,f], E. Teodorescu[29], F. Teubert[38], C. Thomas[55], E. Thomas[38], J. van Tilburg[11], V. Tisserand[4], M. Tobin[39], S. Tolk[42], L. Tomassetti[16,f], D. Tonelli[38], S. Topp-Joergensen[55], N. Torr[55], E. Tournefier[4,53], S. Tourneur[39], M.T. Tran[39], M. Tresch[40], A. Tsaregorodtsev[6], P. Tsopelas[41], N. Tuning[41], M. Ubeda Garcia[38], A. Ukleja[28], A. Ustyuzhanin[62], U. Uwer[11], V. Vagnoni[14], G. Valenti[14], A. Vallier[7], R. Vazquez Gomez[18], P. Vazquez Regueiro[37], C. Vázquez Sierra[37], S. Vecchi[16], J.J. Velthuis[46], M. Veltri[17,h], G. Veneziano[39], M. Vesterinen[11], B. Viaud[7], D. Vieira[2], X. Vilasis-Cardona[36,p], A. Vollhardt[40], D. Volyanskyy[10], D. Voong[46], A. Vorobyev[30], V. Vorobyev[34], C. Voß[61], H. Voss[10], J.A. de Vries[41], R. Waldi[61], C. Wallace[48], R. Wallace[12], S. Wandernoth[11], J. Wang[59], D.R. Ward[47], N.K. Watson[45], A.D. Webber[54], D. Websdale[53], M. Whitehead[48], J. Wicht[38], J. Wiechczynski[26], D. Wiedner[11], L. Wiggers[41], G. Wilkinson[55], M.P. Williams[48,49], M. Williams[56], F.F. Wilson[49], J. Wimberley[58], J. Wishahi[9], W. Wislicki[28], M. Witek[26], G. Wormser[7], S.A. Wotton[47], S. Wright[47], S. Wu[3], K. Wyllie[38], Y. Xie[50,38], Z. Xing[59], Z. Yang[3], X. Yuan[3], O. Yushchenko[35], M. Zangoli[14], M. Zavertyaev[10,b], F. Zhang[3], L. Zhang[59], W.C. Zhang[12], Y. Zhang[3], A. Zhelezov[11], A. Zhokhov[31], L. Zhong[3], A. Zvyagin[38].

[1] *Centro Brasileiro de Pesquisas Físicas (CBPF), Rio de Janeiro, Brazil*
[2] *Universidade Federal do Rio de Janeiro (UFRJ), Rio de Janeiro, Brazil*
[3] *Center for High Energy Physics, Tsinghua University, Beijing, China*
[4] *LAPP, Université de Savoie, CNRS/IN2P3, Annecy-Le-Vieux, France*
[5] *Clermont Université, Université Blaise Pascal, CNRS/IN2P3, LPC, Clermont-Ferrand, France*
[6] *CPPM, Aix-Marseille Université, CNRS/IN2P3, Marseille, France*
[7] *LAL, Université Paris-Sud, CNRS/IN2P3, Orsay, France*
[8] *LPNHE, Université Pierre et Marie Curie, Université Paris Diderot, CNRS/IN2P3, Paris, France*
[9] *Fakultät Physik, Technische Universität Dortmund, Dortmund, Germany*
[10] *Max-Planck-Institut für Kernphysik (MPIK), Heidelberg, Germany*
[11] *Physikalisches Institut, Ruprecht-Karls-Universität Heidelberg, Heidelberg, Germany*
[12] *School of Physics, University College Dublin, Dublin, Ireland*
[13] *Sezione INFN di Bari, Bari, Italy*
[14] *Sezione INFN di Bologna, Bologna, Italy*
[15] *Sezione INFN di Cagliari, Cagliari, Italy*
[16] *Sezione INFN di Ferrara, Ferrara, Italy*
[17] *Sezione INFN di Firenze, Firenze, Italy*
[18] *Laboratori Nazionali dell'INFN di Frascati, Frascati, Italy*
[19] *Sezione INFN di Genova, Genova, Italy*
[20] *Sezione INFN di Milano Bicocca, Milano, Italy*
[21] *Sezione INFN di Milano, Milano, Italy*
[22] *Sezione INFN di Padova, Padova, Italy*
[23] *Sezione INFN di Pisa, Pisa, Italy*
[24] *Sezione INFN di Roma Tor Vergata, Roma, Italy*

[25] *Sezione INFN di Roma La Sapienza, Roma, Italy*
[26] *Henryk Niewodniczanski Institute of Nuclear Physics Polish Academy of Sciences, Kraków, Poland*
[27] *AGH - University of Science and Technology, Faculty of Physics and Applied Computer Science, Kraków, Poland*
[28] *National Center for Nuclear Research (NCBJ), Warsaw, Poland*
[29] *Horia Hulubei National Institute of Physics and Nuclear Engineering, Bucharest-Magurele, Romania*
[30] *Petersburg Nuclear Physics Institute (PNPI), Gatchina, Russia*
[31] *Institute of Theoretical and Experimental Physics (ITEP), Moscow, Russia*
[32] *Institute of Nuclear Physics, Moscow State University (SINP MSU), Moscow, Russia*
[33] *Institute for Nuclear Research of the Russian Academy of Sciences (INR RAN), Moscow, Russia*
[34] *Budker Institute of Nuclear Physics (SB RAS) and Novosibirsk State University, Novosibirsk, Russia*
[35] *Institute for High Energy Physics (IHEP), Protvino, Russia*
[36] *Universitat de Barcelona, Barcelona, Spain*
[37] *Universidad de Santiago de Compostela, Santiago de Compostela, Spain*
[38] *European Organization for Nuclear Research (CERN), Geneva, Switzerland*
[39] *Ecole Polytechnique Fédérale de Lausanne (EPFL), Lausanne, Switzerland*
[40] *Physik-Institut, Universität Zürich, Zürich, Switzerland*
[41] *Nikhef National Institute for Subatomic Physics, Amsterdam, The Netherlands*
[42] *Nikhef National Institute for Subatomic Physics and VU University Amsterdam, Amsterdam, The Netherlands*
[43] *NSC Kharkiv Institute of Physics and Technology (NSC KIPT), Kharkiv, Ukraine*
[44] *Institute for Nuclear Research of the National Academy of Sciences (KINR), Kyiv, Ukraine*
[45] *University of Birmingham, Birmingham, United Kingdom*
[46] *H.H. Wills Physics Laboratory, University of Bristol, Bristol, United Kingdom*
[47] *Cavendish Laboratory, University of Cambridge, Cambridge, United Kingdom*
[48] *Department of Physics, University of Warwick, Coventry, United Kingdom*
[49] *STFC Rutherford Appleton Laboratory, Didcot, United Kingdom*
[50] *School of Physics and Astronomy, University of Edinburgh, Edinburgh, United Kingdom*
[51] *School of Physics and Astronomy, University of Glasgow, Glasgow, United Kingdom*
[52] *Oliver Lodge Laboratory, University of Liverpool, Liverpool, United Kingdom*
[53] *Imperial College London, London, United Kingdom*
[54] *School of Physics and Astronomy, University of Manchester, Manchester, United Kingdom*
[55] *Department of Physics, University of Oxford, Oxford, United Kingdom*
[56] *Massachusetts Institute of Technology, Cambridge, MA, United States*
[57] *University of Cincinnati, Cincinnati, OH, United States*
[58] *University of Maryland, College Park, MD, United States*
[59] *Syracuse University, Syracuse, NY, United States*
[60] *Pontifícia Universidade Católica do Rio de Janeiro (PUC-Rio), Rio de Janeiro, Brazil, associated to* [2]
[61] *Institut für Physik, Universität Rostock, Rostock, Germany, associated to* [11]
[62] *National Research Centre Kurchatov Institute, Moscow, Russia, associated to* [31]
[63] *Instituto de Fisica Corpuscular (IFIC), Universitat de Valencia-CSIC, Valencia, Spain, associated to* [36]
[64] *KVI - University of Groningen, Groningen, The Netherlands, associated to* [41]
[65] *Celal Bayar University, Manisa, Turkey, associated to* [38]

[a] *Universidade Federal do Triângulo Mineiro (UFTM), Uberaba-MG, Brazil*
[b] *P.N. Lebedev Physical Institute, Russian Academy of Science (LPI RAS), Moscow, Russia*
[c] *Università di Bari, Bari, Italy*
[d] *Università di Bologna, Bologna, Italy*
[e] *Università di Cagliari, Cagliari, Italy*
[f] *Università di Ferrara, Ferrara, Italy*
[g] *Università di Firenze, Firenze, Italy*
[h] *Università di Urbino, Urbino, Italy*

[i] *Università di Modena e Reggio Emilia, Modena, Italy*
[j] *Università di Genova, Genova, Italy*
[k] *Università di Milano Bicocca, Milano, Italy*
[l] *Università di Roma Tor Vergata, Roma, Italy*
[m] *Università di Roma La Sapienza, Roma, Italy*
[n] *Università della Basilicata, Potenza, Italy*
[o] *AGH - University of Science and Technology, Faculty of Computer Science, Electronics and Telecommunications, Kraków, Poland*
[p] *LIFAELS, La Salle, Universitat Ramon Llull, Barcelona, Spain*
[q] *Hanoi University of Science, Hanoi, Viet Nam*
[r] *Università di Padova, Padova, Italy*
[s] *Università di Pisa, Pisa, Italy*
[t] *Scuola Normale Superiore, Pisa, Italy*
[u] *Università degli Studi di Milano, Milano, Italy*

1 Introduction

Studies of the production of heavy quark-antiquark bound systems, such as the $b\bar{b}$ states $\Upsilon(1S)$, $\Upsilon(2S)$ and $\Upsilon(3S)$ (indicated generically as Υ in the following) in hadron-hadron interactions probe the dynamics of the colliding partons and provide a unique insight into quantum chromodynamics (QCD). The total production cross-sections and spin configurations of these heavy quarkonium states are currently not reproduced by the theoretical models. These include the colour singlet model [1–5], recently improved by adding higher-order contributions [6, 7], the colour-evaporation model [8], and the non-perturbative colour octet mechanism [9–11], which is investigated in the framework of non-relativistic QCD. The first complete next-to-leading order calculation of Υ production properties [12], based on the non-relativistic QCD factorisation scheme, provides a good description of the measured differential cross-sections at large transverse momentum, $p_{\rm T}$, but overestimates the data at low $p_{\rm T}$.

The production of Υ mesons in proton-proton (pp) collisions occurs either directly in parton scattering or via feed-down from the decay of heavier prompt bottomonium states, like $\chi_{\rm b}$ [13–16], or higher-mass Υ states. The latter source complicates the theoretical description of bottomonium production [17, 18].

The Large Hadron Collider provides a unique possibility to study bottomonium and charmonium hadroproduction in pp interactions at different collision energies and discriminate between various theoretical approaches. This study presents the first measurement of the inclusive production cross-sections of the three considered Υ mesons in pp collisions at a centre-of-mass energy of $\sqrt{s} = 2.76\,\text{TeV}$. The measurements are performed as functions of the Υ transverse momentum and rapidity, y, separately in six bins of $p_{\rm T}$ in the range $p_{\rm T} < 15\,\text{GeV}/c$ and five bins of y in the range $2.0 < y < 4.5$. The results are reported as products of the cross-sections and the branching fractions of Υ mesons into the dimuon final state. This analysis is complementary to those performed by the ATLAS [19], CMS [20] and LHCb [21, 22] collaborations and allows studies of the Υ production cross-section at forward rapidities as a function of the centre-of-mass energy.

2 Detector and data sample

The LHCb detector [23] is a single-arm forward spectrometer covering the pseudorapidity range $2 < \eta < 5$, designed for the study of particles containing b or c quarks. The detector includes a high-precision tracking system consisting of a silicon-strip vertex detector surrounding the pp interaction region, a large-area silicon-strip detector located upstream of a dipole magnet with a bending power of about 4 Tm, and three stations of silicon-strip detectors and straw drift tubes placed downstream. The combined tracking system provides a momentum measurement with relative uncertainty that varies from 0.4% at $5\,\text{GeV}/c$ to 0.6% at $100\,\text{GeV}/c$, and impact parameter resolution of $20\,\mu\text{m}$ for tracks with large transverse momentum. Different types of charged hadrons are distinguished by information from two ring-imaging Cherenkov detectors [24]. Photon, electron and hadron candidates are identified by a calorimeter system consisting of scintillating-pad and

preshower detectors, an electromagnetic calorimeter and a hadronic calorimeter. Muons are identified by a system composed of alternating layers of iron and multiwire proportional chambers [25].

The analysis is carried out using a sample of data corresponding to an integrated luminosity of $3.3\,\text{pb}^{-1}$ collected in pp collisions at $\sqrt{s} = 2.76\,\text{TeV}$. Events of interest are preselected by a trigger consisting of a hardware stage, based on information from the calorimeter and muon systems, followed by a software stage, which applies a full event reconstruction. The presence of two muon candidates with the product of their p_{T} larger than 1.68 $(\text{GeV}/c)^2$ is required in the hardware trigger. At the software stage, the events are required to contain two well reconstructed tracks with hits in the muon system, having total and transverse momenta greater than $6\,\text{GeV}/c$ and $0.5\,\text{GeV}/c$, respectively. The selected muon candidates are further required to originate from a common vertex and have an invariant mass larger than $4.7\,\text{GeV}/c^2$.

To determine the acceptance, reconstruction and trigger efficiencies, fully simulated signal samples are reweighted to reproduce the multiplicity distributions for reconstructed primary vertices, tracks and hits in the detector observed in the data. The simulation is performed using the LHCb configuration [26] of the Pythia 6.4 event generator [27]. Here, decays of hadronic particles are described by EvtGen [28] in which final-state photons are generated using Photos [29]. The interaction of the generated particles with the detector and its response are implemented using the Geant4 toolkit [30, 31] as described in Ref. [32].

3 Signal selection and cross-section determination

The selection strategy used in the previous LHCb studies on Υ production [21,22] is applied here. It includes selection criteria that ensure good quality track and vertex reconstruction. In addition, the muon candidates are required to have $p > 10\,\text{GeV}/c$ and $p_{\text{T}} > 1\,\text{GeV}/c$. To further reduce background contamination, a set of additional requirements is employed in this analysis. It consists of tightened criteria on track quality [33], muon identification [34] and a good quality of a global fit of the dimuon vertex with a primary vertex constraint [35].

The invariant mass distribution of the selected $\Upsilon \to \mu^+\mu^-$ candidates is shown in Fig. 1 for the full kinematic range. The distribution is described by a function similar to the one used in the previous studies on Υ production [21,22]. It models the signal component using the sum of three Crystal Ball functions [36], one for each of the $\Upsilon(1S)$, $\Upsilon(2S)$ and $\Upsilon(3S)$ signals, and includes an exponential component to account for combinatorial background. The position and width of the Crystal Ball function describing the $\Upsilon(1S)$ meson are allowed to vary, while the mass differences between Υ states are fixed to their known values [37] along with parameters describing the radiative tail, as determined from simulation studies. The widths of the $\Upsilon(2S)$ and $\Upsilon(3S)$ peaks are constrained to the value of the width of the $\Upsilon(1S)$ signal scaled by the ratio of their masses to the $\Upsilon(1S)$ mass. In total, five parameters are extracted from the fit for the signal component: the yields of $\Upsilon(1S)$, $\Upsilon(2S)$ and $\Upsilon(3S)$ states, the $\Upsilon(1S)$ mass resolution and its peak position. The latter is found to

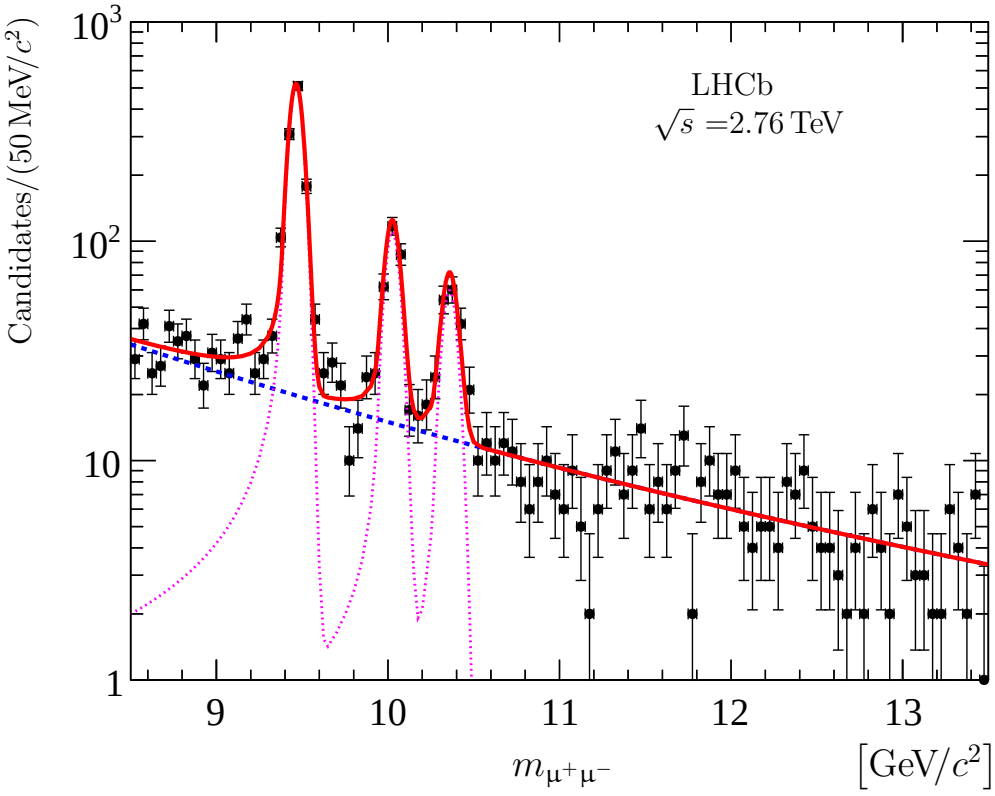

Figure 1: Invariant mass distribution of selected $\Upsilon \to \mu^+\mu^-$ candidates with $p_{\rm T} < 15\,{\rm GeV}/c$ and $2.0 < y < 4.5$. The result of the fit described in the text is illustrated with a red solid line, while the signal and background components are shown with magenta dotted and blue dashed lines, respectively. The three peaks correspond to the $\Upsilon(1S)$, $\Upsilon(2S)$ and $\Upsilon(3S)$ mesons (from left to right).

be consistent with the known mass of the $\Upsilon(1S)$ meson [37], while reasonable agreement is observed between the data and simulation for the $\Upsilon(1S)$ mass resolution.

The Υ production cross-sections are measured separately in six bins of $p_{\rm T}$ and five bins of y since the limited amount of data does not allow a measurement of double differential cross-sections. For a given $p_{\rm T}$ or y bin, the differential cross-section for the inclusive Υ production of the three different states decaying into the dimuon final state is determined as

$$\frac{{\rm d}\sigma\left({\rm pp} \to \Upsilon {\rm X}\right)}{{\rm d}p_{\rm T}} \times \mathcal{B}\left(\Upsilon \to \mu^+\mu^-\right) = \frac{N_\Upsilon^{\rm corr}}{\mathcal{L} \times \Delta p_{\rm T}}\,, \tag{1a}$$

$$\frac{{\rm d}\sigma\left({\rm pp} \to \Upsilon {\rm X}\right)}{{\rm d}y} \times \mathcal{B}\left(\Upsilon \to \mu^+\mu^-\right) = \frac{N_\Upsilon^{\rm corr}}{\mathcal{L} \times \Delta y}\,, \tag{1b}$$

where $N_\Upsilon^{\rm corr}$ is the efficiency-corrected yield of $\Upsilon \to \mu^+\mu^-$ decays, $\mathcal{L}$ stands for the integrated luminosity and $\Delta p_{\rm T}\,(\Delta y)$ denotes the $p_{\rm T}\,(y)$ bin size. For the mass fits in individual

$p_{\rm T}$ and y bins, the $\Upsilon(1S)$ peak position is fixed to the value obtained from the fit for the full kinematic range, while the $\Upsilon(1S)$ mass resolution is parameterised with a function of $p_{\rm T}$ and y using simulation. The total observed signal yields and their statistical uncertainties for $\Upsilon(1S)$, $\Upsilon(2S)$ and $\Upsilon(3S)$ mesons obtained by summation over $p_{\rm T}\,(y)$ bins are $1139\pm37\,(1145\pm37)$, $271\pm20\,(270\pm20)$ and $158\pm16\,(156\pm16)$, respectively. These results are in good agreement with the total signal yields obtained from the fit to the reconstructed dimuon invariant mass for the full kinematic range.

Based on the mass fit results in individual bins, the efficiency-corrected yield for each kinematic region is determined as

$$N_{\Upsilon}^{\rm corr} = \sum_i \frac{w_i^{\Upsilon}}{\varepsilon_i^{\rm tot}} \,, \tag{2}$$

where w_i^{Υ} is a signal weight factor, $\varepsilon_i^{\rm tot}$ is the total signal event efficiency and the sum runs over all candidates i. The w_i^{Υ} factor accounts for the background subtraction and is obtained from the fit using the *sPlot* technique [38]. The total signal event efficiency is calculated for each $\Upsilon\to\mu^+\mu^-$ candidate as

$$\varepsilon^{\rm tot} = \varepsilon^{\rm acc}\times\varepsilon^{\rm rec}\times\varepsilon^{\rm trg}\times\varepsilon^{\mu{\rm ID}} \,, \tag{3}$$

where $\varepsilon^{\rm acc}$ is the detector acceptance, $\varepsilon^{\rm rec}$ is the reconstruction and selection efficiency, $\varepsilon^{\rm trg}$ is the trigger efficiency and $\varepsilon^{\mu{\rm ID}}$ is the efficiency of muon identification. The efficiencies $\varepsilon^{\rm acc}$, $\varepsilon^{\rm rec}$ and $\varepsilon^{\rm trg}$ are determined using simulation and further corrected using data-driven techniques to account for small differences in muon reconstruction efficiency between data and simulation [33, 34, 39]. The efficiency $\varepsilon^{\mu{\rm ID}}$ is measured directly from data using a tag-and-probe method on a large sample of $J/\psi\to\mu^+\mu^-$ decays. The total efficiency-corrected signal yields obtained by summation over $p_{\rm T}\,(y)$ bins for $\Upsilon(1S)$, $\Upsilon(2S)$ and $\Upsilon(3S)$ mesons are $3678\pm144\,(3684\pm143)$, $875\pm76\,(869\pm75)$ and $527\pm65\,(515\pm64)$, respectively.

The integrated luminosity of the data sample is estimated with the beam-gas imaging method [40–44]. It is based on the beam currents and the measurements of the angles, offsets and transverse profiles of the two colliding bunches, which is achieved by reconstructing beam-gas interaction vertices.

4 Systematic uncertainties

Previous LHCb studies of Υ production [21, 22] showed that the signal efficiency depends on the initial polarisation of Υ mesons. This property was measured in pp collisions at $\sqrt{s} = 7\,{\rm TeV}$ by the CMS collaboration at central rapidities and large $p_{\rm T}$ and was found to be small [45]. Polarisation of other vector quarkonium states, such as J/ψ and $\psi(2S)$ mesons was studied in pp collisions at $\sqrt{s} = 7\,{\rm TeV}$ by the LHCb [46, 47] and ALICE [48] collaborations and was also found to be small. This analysis is performed assuming zero polarisation of Υ mesons and no corresponding systematic uncertainty is assigned.

Table 1: Relative systematic uncertainties (in %) affecting the Υ production cross-section measurements in the full kinematic region. The total uncertainties are obtained by adding the individual effects in quadrature.

Source	Υ(1S)	Υ(2S)	Υ(3S)
Luminosity	2.3	2.3	2.3
Fit model and range	0.5	1.0	2.3
Data-simulation agreement			
Radiative tails	1.0	1.0	1.0
Multiplicity reweighting	0.6	0.4	2.0
Efficiency corrections	0.7	1.0	1.0
Track reconstruction	2×0.4	2×0.4	2×0.4
Selection variables	1.0	1.0	1.0
Trigger	2.0	2.0	2.0
Total	3.6	3.7	4.7

The systematic uncertainties affecting the Υ cross-section measurements presented in this paper are summarised in Table 1. These uncertainties are strongly correlated between bins. The largest contribution arises from the absolute luminosity scale, which is determined with a 2.3% uncertainty. It is dominated by the vertex resolution of beam-gas interactions and detector alignment [44].

The influence of the signal extraction technique is studied by varying the fit range and the signal and background parameterisations used in the fit model. The fits are also performed with floating mass and resolution of the Υ(1S) peak and without constraints for the Υ(2S) and Υ(3S) masses. The spread of the extracted signal yields between these scenarios is taken as the corresponding systematic uncertainty. It ranges from 0.4 to 33% for different $p_{\rm T}\,(y)$ bins and amounts to 0.5%, 1.0% and 2.3% for the Υ(1S), Υ(2S) and Υ(3S) cross-section measurements in the full kinematic region, respectively.

The possible mismodeling of bremsstrahlung simulation for the radiative tail and its effect on the signal shape was addressed in the previous LHCb analysis [22]. It leads to an additional uncertainty of 1.0%.

Several systematic uncertainties are related to the determination of the total efficiency components in Eq. (3). The detector acceptance, reconstruction and selection efficiencies are determined using simulated samples. These are corrected using an iterative procedure to match the multiplicity distributions for reconstructed primary vertices, tracks and hits in the detector with those observed in data. The systematic uncertainty associated with this reweighting procedure is assessed by varying the number of iterative steps. It ranges from 0.4 to 4.8% for different $p_{\rm T}\,(y)$ bins and is found to be 0.6%, 0.4% and 2.0% for the Υ(1S), Υ(2S) and Υ(3S) cross-section measurements in the full kinematic region, respectively.

The $\varepsilon^{\rm rec}$ efficiency is corrected using data-driven techniques for a small difference in the muon reconstruction efficiency between data and simulation [33,34]. The $\varepsilon^{\rm \mu ID}$ efficiency

is determined from data using alternative methods, based on a tag-and-probe approach on a large sample of $J/\psi \to \mu^+\mu^-$ decays. The difference between these methods is taken as the corresponding systematic uncertainty. It is combined with the uncertainties associated with the correction factors discussed above and propagated to the Υ cross-section measurements using 400 pseudo-experiments. The resulting uncertainty ranges from 1.0 to 13% for different p_{T} (y) bins and amounts to 0.7%, 1.0% and 1.0% for the $\Upsilon(1S)$, $\Upsilon(2S)$ and $\Upsilon(3S)$ cross-section measurements in the full kinematic region, respectively.

To account for differences between the actual tracking efficiency and that estimated with simulation using data-driven techniques [33, 39], a systematic uncertainty of 0.4% is assigned per track.

Good agreement between the data and reweighted simulation is observed for all selection variables used in this analysis, in particular for the χ^2 of the dimuon vertex fit and the χ^2 of the global fit [35]. The discrepancies do not exceed 1.0%, which is conservatively taken as a systematic uncertainty to account for the disagreement between the data and simulation.

The systematic uncertainty associated with the trigger requirements is assessed by studying the performance of the dimuon trigger, described in Sect. 2, for events selected using the single muon high-p_{T} trigger [49]. The fractions of signal $\Upsilon(1S)$ events selected using both trigger requirements are compared for the data and simulation in bins of dimuon p_{T}, and a systematic uncertainty of 2.0% is assigned.

5 Results

The integrated Υ production cross-sections times dimuon branching fractions in the kinematic region $p_{\mathrm{T}} < 15\,\mathrm{GeV}/c$ and $2.0 < y < 4.5$ are measured to be

$$\begin{aligned}
\sigma\left(\mathrm{pp} \to \Upsilon(1S)\mathrm{X}\right) \times \mathcal{B}\left(\Upsilon(1S) \to \mu^+\mu^-\right) &= 1.111 \pm 0.043 \pm 0.044\,\mathrm{nb}, \\
\sigma\left(\mathrm{pp} \to \Upsilon(2S)\mathrm{X}\right) \times \mathcal{B}\left(\Upsilon(2S) \to \mu^+\mu^-\right) &= 0.264 \pm 0.023 \pm 0.011\,\mathrm{nb}, \\
\sigma\left(\mathrm{pp} \to \Upsilon(3S)\mathrm{X}\right) \times \mathcal{B}\left(\Upsilon(3S) \to \mu^+\mu^-\right) &= 0.159 \pm 0.020 \pm 0.007\,\mathrm{nb},
\end{aligned}$$

where the first uncertainty is statistical and the second systematic.

The single differential cross-sections times dimuon branching fractions are shown as functions of p_{T} and y in Fig. 2 and summarised in Table 2. The total uncertainties of the results are dominated by statistical effects in all p_{T} and y bins. In addition to the data, Fig. 2 reports theoretical predictions, based on the next-to-leading order non-relativistic QCD calculation [18], for the Υ differential cross-sections in the kinematic region $6 < p_{\mathrm{T}} < 15\,\mathrm{GeV}/c$ and $2.0 < y < 4.5$. The long-distance matrix elements used in the calculations are fitted to CDF [50] and D0 [51] results for $\Upsilon(1S)$ production in $\mathrm{p\overline{p}}$ collisions at $\sqrt{s} = 1.8$ and 1.96 TeV. The predictions include the feed-down contributions from higher excited S-wave and P-wave $\mathrm{b\overline{b}}$ states. Good agreement between the data and predictions is found for all three Υ states. The dependence of the Υ cross-sections on y is found to be more pronounced than at higher collision energies [21, 22], which is in line with theoretical expectations presented for example in Ref. [52].

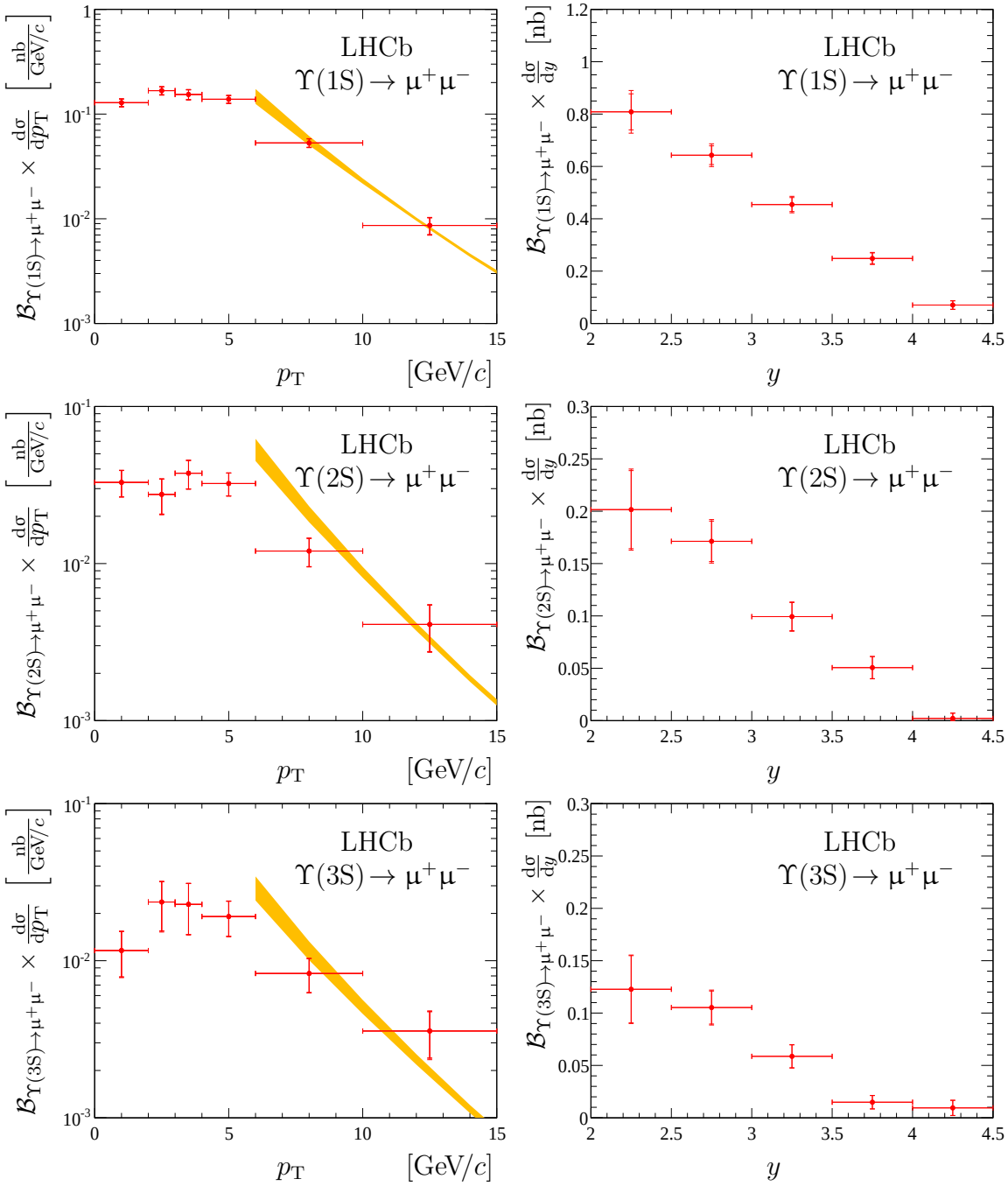

Figure 2: Differential cross-sections for $\Upsilon(1S)$, $\Upsilon(2S)$ and $\Upsilon(3S)$ mesons times dimuon branching fractions as functions of p_T (left) and y (right). The inner error bars indicate the statistical uncertainty, while the outer error bars indicate the sum of statistical and systematic uncertainties in quadrature. The next-to-leading order non-relativistic QCD predictions [18] are shown by the solid yellow band.

Table 2: Cross-sections for Υ(1S), Υ(2S) and Υ(3S) mesons times dimuon branching fractions (in nb) in bins of p_{T} and y without normalisation to the bin sizes. The first uncertainty is statistical and the second is systematic.

p_{T} [GeV/c]	$\Upsilon(1\mathrm{S}) \to \mu^+\mu^-$	$\Upsilon(2\mathrm{S}) \to \mu^+\mu^-$	$\Upsilon(3\mathrm{S}) \to \mu^+\mu^-$
0–2	$0.257 \pm 0.021 \pm 0.011$	$0.066 \pm 0.012 \pm 0.007$	$0.023 \pm 0.007 \pm 0.002$
2–3	$0.167 \pm 0.014 \pm 0.007$	$0.028 \pm 0.007 \pm 0.002$	$0.024 \pm 0.008 \pm 0.002$
3–4	$0.154 \pm 0.016 \pm 0.009$	$0.038 \pm 0.008 \pm 0.002$	$0.023 \pm 0.008 \pm 0.001$
4–6	$0.277 \pm 0.023 \pm 0.013$	$0.065 \pm 0.011 \pm 0.003$	$0.038 \pm 0.010 \pm 0.002$
6–10	$0.212 \pm 0.019 \pm 0.008$	$0.048 \pm 0.010 \pm 0.002$	$0.033 \pm 0.008 \pm 0.001$
10–15	$0.043 \pm 0.008 \pm 0.003$	$0.020 \pm 0.007 \pm 0.001$	$0.018 \pm 0.006 \pm 0.002$

y	$\Upsilon(1\mathrm{S}) \to \mu^+\mu^-$	$\Upsilon(2\mathrm{S}) \to \mu^+\mu^-$	$\Upsilon(3\mathrm{S}) \to \mu^+\mu^-$
2.0–2.5	$0.404 \pm 0.034 \pm 0.022$	$0.101 \pm 0.019 \pm 0.005$	$0.061 \pm 0.016 \pm 0.003$
2.5–3.0	$0.321 \pm 0.018 \pm 0.012$	$0.086 \pm 0.010 \pm 0.004$	$0.053 \pm 0.008 \pm 0.003$
3.0–3.5	$0.227 \pm 0.013 \pm 0.008$	$0.050 \pm 0.007 \pm 0.002$	$0.029 \pm 0.005 \pm 0.001$
3.5–4.0	$0.124 \pm 0.011 \pm 0.005$	$0.025 \pm 0.005 \pm 0.001$	$0.007 \pm 0.003 \pm 0.001$
4.0–4.5	$0.035 \pm 0.008 \pm 0.002$	$0.001 \pm 0.003 \pm 0.001$	$0.005 \pm 0.004 \pm 0.001$

Table 3: Ratios of the Υ(2S) to Υ(1S) and Υ(3S) to Υ(1S) cross-sections times dimuon branching fractions as functions of p_{T} and y. The first uncertainty is statistical and the second is systematic.

p_{T} [GeV/c]	$\mathcal{R}^{2S/1S}$	$\mathcal{R}^{3S/1S}$
0–2	$0.257 \pm 0.053 \pm 0.009$	$0.090 \pm 0.030 \pm 0.006$
2–3	$0.165 \pm 0.044 \pm 0.007$	$0.141 \pm 0.050 \pm 0.010$
3–4	$0.244 \pm 0.056 \pm 0.007$	$0.148 \pm 0.055 \pm 0.006$
4–6	$0.233 \pm 0.043 \pm 0.007$	$0.138 \pm 0.037 \pm 0.005$
6–10	$0.227 \pm 0.051 \pm 0.006$	$0.157 \pm 0.041 \pm 0.004$
10–15	$0.474 \pm 0.179 \pm 0.031$	$0.413 \pm 0.155 \pm 0.029$

y		
2.0–2.5	$0.249 \pm 0.051 \pm 0.007$	$0.152 \pm 0.042 \pm 0.006$
2.5–3.0	$0.266 \pm 0.033 \pm 0.007$	$0.164 \pm 0.026 \pm 0.007$
3.0–3.5	$0.219 \pm 0.032 \pm 0.004$	$0.129 \pm 0.025 \pm 0.003$
3.5–4.0	$0.204 \pm 0.046 \pm 0.004$	$0.060 \pm 0.026 \pm 0.003$

Figure 3 illustrates the ratios of the Υ(2S) to Υ(1S), $\mathcal{R}^{2S/1S}$, and Υ(3S) to Υ(1S), $\mathcal{R}^{3S/1S}$, cross-sections times dimuon branching fractions as functions of p_{T} and y. Here, most of the systematic uncertainties on the cross-sections cancel, while the statistical uncertainties remain significant. The ratios are found to be in good agreement with the corresponding results obtained in the previous analyses on Υ production at $\sqrt{s} = 7$ and 8 TeV [21, 22]. The measured $\mathcal{R}^{2S/1S}$ and $\mathcal{R}^{3S/1S}$ are also consistent with theoretical predictions presented in Refs. [52–54], where the Υ(3S) meson is considered as a mixture

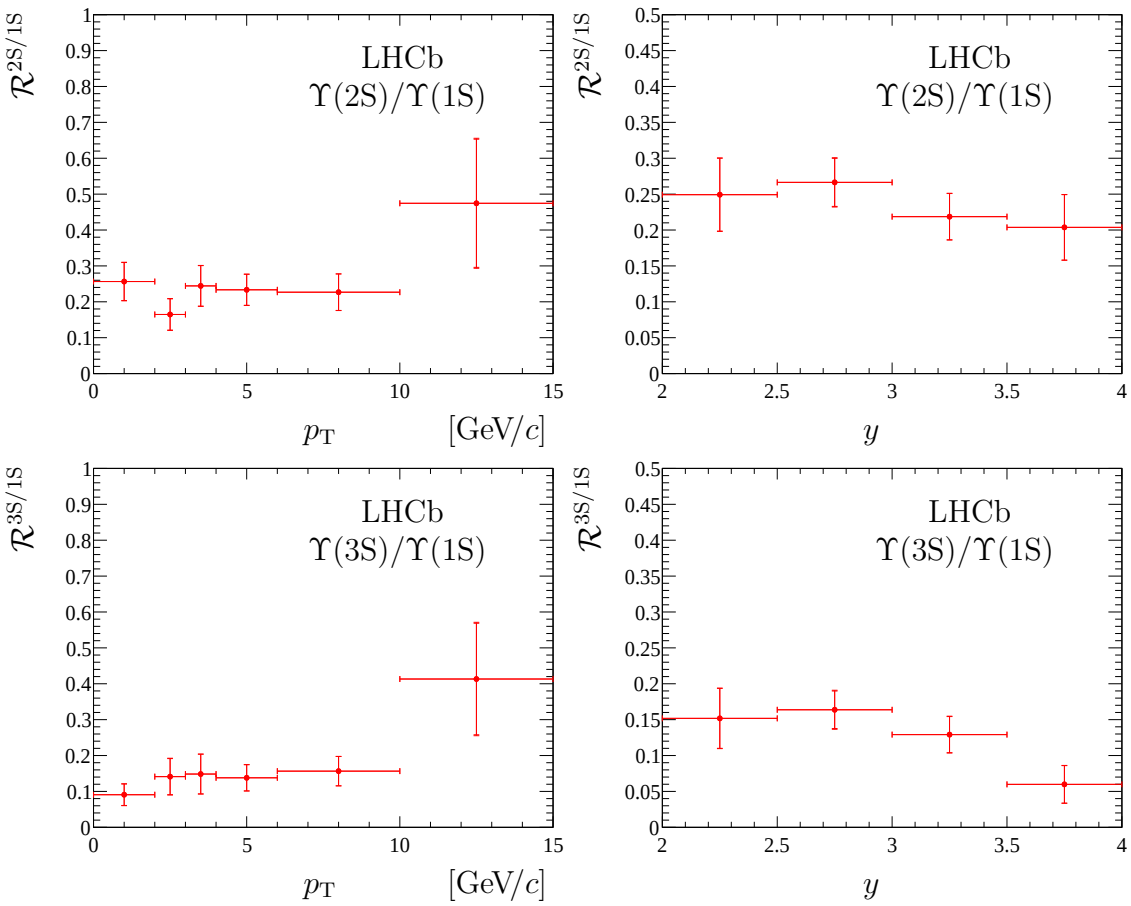

Figure 3: Ratios of the $\Upsilon(2S)$ to $\Upsilon(1S)$ and $\Upsilon(3S)$ to $\Upsilon(1S)$ cross-sections times dimuon branching fractions as functions of p_T and y. The error bars indicate the total uncertainties of the results obtained by adding statistical and systematic uncertainties in quadrature.

of normal $b\bar{b}$ and hybrid $b\bar{b}g$ states. Table 3 lists $\mathcal{R}^{2S/1S}$ and $\mathcal{R}^{3S/1S}$ for each p_T and y bin.

To provide a reference for a future LHCb measurement of Υ production with pPb collisions at $\sqrt{s_{NN}} = 5$ TeV, the Υ cross-sections are measured in the reduced kinematic region $p_T < 15\,\text{GeV}/c$ and $2.5 < y < 4.0$. The corresponding integrated cross-sections times dimuon branching fractions in this kinematic region are

$$\begin{aligned}
\sigma\left(pp \to \Upsilon(1S)X\right) \times \mathcal{B}\left(\Upsilon(1S) \to \mu^+\mu^-\right) &= 0.670 \pm 0.025 \pm 0.026\,\text{nb}, \\
\sigma\left(pp \to \Upsilon(2S)X\right) \times \mathcal{B}\left(\Upsilon(2S) \to \mu^+\mu^-\right) &= 0.159 \pm 0.013 \pm 0.007\,\text{nb}, \\
\sigma\left(pp \to \Upsilon(3S)X\right) \times \mathcal{B}\left(\Upsilon(3S) \to \mu^+\mu^-\right) &= 0.089 \pm 0.010 \pm 0.004\,\text{nb}.
\end{aligned}$$

6 Conclusions

The production of $\Upsilon(1S)$, $\Upsilon(2S)$ and $\Upsilon(3S)$ mesons is observed for the first time in pp collisions at a centre-of-mass energy of $\sqrt{s} = 2.76\,\text{TeV}$ at forward rapidities with a data sample corresponding to an integrated luminosity of $3.3\,\text{pb}^{-1}$. The Υ differential production cross-sections times dimuon branching fractions are measured separately as functions of the Υ transverse momentum and rapidity for $p_{\text{T}} < 15\,\text{GeV}/c$ and $2.0 < y < 4.5$. The theoretical predictions, based on the next-to-leading order non-relativistic QCD calculation, provide a good description of the data at large p_{T}. The ratios of the $\Upsilon(2S)$ to $\Upsilon(1S)$ and $\Upsilon(3S)$ to $\Upsilon(1S)$ cross-sections times dimuon branching fractions as functions of p_{T} and y are found to be in agreement with the corresponding results obtained at higher collision energies.

Acknowledgements

We thank G. Bodwin, L. S. Kisslinger, A. K. Likhoded and A. V. Luchinsky for fruitful discussions about bottomonium production. In addition, we are grateful to K.-T. Chao, H. Han and H.-S. Shao for the next-to-leading order non-relativistic QCD predictions for prompt Υ production at $\sqrt{s} = 2.76\,\text{TeV}$. We also express our gratitude to our colleagues in the CERN accelerator departments for the excellent performance of the LHC. We thank the technical and administrative staff at the LHCb institutes. We acknowledge support from CERN and from the national agencies: CAPES, CNPq, FAPERJ and FINEP (Brazil); NSFC (China); CNRS/IN2P3 and Region Auvergne (France); BMBF, DFG, HGF and MPG (Germany); SFI (Ireland); INFN (Italy); FOM and NWO (The Netherlands); SCSR (Poland); MEN/IFA (Romania); MinES, Rosatom, RFBR and NRC "Kurchatov Institute" (Russia); MinECo, XuntaGal and GENCAT (Spain); SNSF and SER (Switzerland); NAS Ukraine (Ukraine); STFC (United Kingdom); NSF (USA). We also acknowledge the support received from the ERC under FP7. The Tier1 computing centres are supported by IN2P3 (France), KIT and BMBF (Germany), INFN (Italy), NWO and SURF (The Netherlands), PIC (Spain), GridPP (United Kingdom). We are indebted to the communities behind the multiple open source software packages we depend on. We are also thankful for the computing resources and the access to software R&D tools provided by Yandex LLC (Russia).

References

[1] V. G. Kartvelishvili, A. K. Likhoded, and S. R. Slabospitsky, D *meson and* ψ *meson production in hadronic interactions*, Sov. J. Nucl. Phys. **28** (1978) 678.

[2] C.-H. Chang, *Hadronic production of* J/ψ *associated with a gluon*, Nucl. Phys. **B172** (1980) 425.

[3] E. L. Berger and D. Jones, *Inelastic photoproduction of* J/ψ *and* Υ *by gluons*, Phys. Rev. **D23** (1981) 1521.

[4] R. Baier and R. Rückl, *Hadronic collisions: a quarkonium factory*, Z. Phys. **C19** (1983) 251.

[5] R. Baier and R. Rückl, *Hadronic production of* J/ψ *and* Υ*: transverse momentum distributions*, Phys. Lett. **B102** (1981) 364.

[6] J. Campbell, F. Maltoni, and F. Tramontano, *QCD corrections to* J/ψ *and* Υ *production at hadron colliders*, Phys. Rev. Lett. **98** (2007) 252002, arXiv:hep-ph/0703113.

[7] P. Artoisenet *et al.*, Υ *production at Fermilab Tevatron and LHC energies*, Phys. Rev. Lett. **101** (2008) 152001, arXiv:0806.3282.

[8] A. D. Frawley, T. Ullrich, and R. Vogt, *Heavy flavor in heavy-ion collisions at RHIC and RHIC II*, Phys. Rept. **462** (2008) 125, arXiv:0806.1013.

[9] G. T. Bodwin, E. Braaten, and G. P. Lepage, *Rigorous QCD analysis of inclusive annihilation and production of heavy quarkonium*, Phys. Rev. **D51** (1995) 1125, arXiv:hep-ph/9407339.

[10] P. Cho and A. K. Leibovich, *Color-octet quarkonia production*, Phys. Rev. **D53** (1996) 150, arXiv:hep-ph/9505329.

[11] P. Cho and A. K. Leibovich, *Color-octet quarkonia production II*, Phys. Rev. **D53** (1996) 6203, arXiv:hep-ph/9511315.

[12] B. Gong, L.-P. Wan, J.-X. Wang, and H.-F. Zhang, *Complete next-to-leading-order study on the yield and polarization of* $\Upsilon(1S, 2S, 3S)$ *at the Tevatron and LHC*, arXiv:1305.0748.

[13] ATLAS collaboration, G. Aad *et al.*, *Observation of a new* χ_b *state in radiative transitions to* $\Upsilon(1S)$ *and* $\Upsilon(2S)$ *at ATLAS*, Phys. Rev. Lett. **108** (2012) 152001, arXiv:1112.5154.

[14] D0 collaboration, V. M. Abazov *et al.*, *Observation of a narrow mass state decaying into* $\Upsilon(1S) + \gamma$ *in* $p\overline{p}$ *collisions at* $\sqrt{s} = 1.96$ *TeV*, Phys. Rev. **D86** (2012) 031103, arXiv:1203.6034.

[15] LHCb collaboration, R. Aaij *et al.*, *Measurement of the fraction of* $\Upsilon(1S)$ *originating from* $\chi_b(1P)$ *decays in* pp *collisions at* $\sqrt{s} = 7\,\text{TeV}$, JHEP **11** (2012) 31, arXiv:1209.0282.

[16] LHCb collaboration, *Observation of* $\chi_b(3P)$ *state at LHCb in* pp *collisions at* $\sqrt{s} = 7\,\text{TeV}$, LHCb-CONF-2012-020.

[17] A. Likhoded, A. Luchinsky, and S. Poslavsky, *Production of χ_b-mesons at LHC*, Phys. Rev. **D86** (2012) 074027, arXiv:1203.4893.

[18] K. Wang, Y.-Q. Ma, and K.-T. Chao, *$\Upsilon(1S)$ prompt production at the Tevatron and LHC in nonrelativistic QCD*, Phys. Rev. **D85** (2012) 114003, arXiv:1202.6012.

[19] ATLAS Collaboration, G. Aad *et al.*, *Measurement of Upsilon production in 7 TeV pp collisions at ATLAS*, Phys. Rev. **D87** (2013) 052004, arXiv:1211.7255.

[20] CMS Collaboration, S. Chatrchyan *et al.*, *Measurement of the $\Upsilon(1S)$, $\Upsilon(2S)$ and $\Upsilon(3S)$ cross sections in pp collisions at $\sqrt{s}$ = 7 TeV*, Phys. Lett. **B727** (2013) 101, arXiv:1303.5900.

[21] LHCb collaboration, R. Aaij *et al.*, *Measurement of Υ production in* pp *collisions at $\sqrt{s} = 7$ TeV*, Eur. Phys. J. **C72** (2012) 2025, arXiv:1202.6579.

[22] LHCb collaboration, R. Aaij *et al.*, *Production of J/ψ and Υ mesons in* pp *collisions at $\sqrt{s} = 8$ TeV*, JHEP **06** (2013) 64, arXiv:1304.6977.

[23] LHCb collaboration, A. A. Alves Jr. *et al.*, *The LHCb detector at the LHC*, JINST **3** (2008) S08005.

[24] M. Adinolfi *et al.*, *Performance of the LHCb RICH detector at the LHC*, Eur. Phys. J. **C73** (2013) 2431, arXiv:1211.6759.

[25] A. A. Alves Jr. *et al.*, *Performance of the LHCb muon system*, JINST **8** (2013) P02022, arXiv:1211.1346.

[26] I. Belyaev *et al.*, *Handling of the generation of primary events in* Gauss*, the LHCb simulation framework*, Nuclear Science Symposium Conference Record (NSS/MIC) **IEEE** (2010) 1155.

[27] T. Sjöstrand, S. Mrenna, and P. Skands, Pythia *6.4 physics and manual*, JHEP **05** (2006) 026, arXiv:hep-ph/0603175.

[28] D. J. Lange, *The* EvtGen *particle decay simulation package*, Nucl. Instrum. Meth. **A462** (2001) 152.

[29] P. Golonka and Z. Was, Photos *Monte Carlo: a precision tool for QED corrections in Z and W decays*, Eur. Phys. J. **C45** (2006) 97, arXiv:hep-ph/0506026.

[30] Geant4 collaboration, J. Allison *et al.*, Geant4 *developments and applications*, IEEE Trans. Nucl. Sci. **53** (2006) 270.

[31] Geant4 collaboration, S. Agostinelli *et al.*, Geant4*: a simulation toolkit*, Nucl. Instrum. Meth. **A506** (2003) 250.

[32] M. Clemencic *et al.*, *The LHCb simulation application,* GAUSS*: design, evolution and experience*, J. Phys. Conf. Ser. **331** (2011) 032023.

[33] R. Aaij *et al.*, *Measurement of the track reconstruction efficiency at LHCb*, LHCb-DP-2013-002, in preparation.

[34] F. Archilli *et al.*, *Performance of the muon identification at LHCb*, JINST **8** (2013) P10020, arXiv:1306.0249.

[35] W. D. Hulsbergen, *Decay chain fitting with a Kalman filter*, Nucl. Instrum. Meth. **A552** (2005) 566, arXiv:physics/0503191.

[36] T. Skwarnicki, *A study of the radiative cascade transitions between the* Υ' *and* Υ *resonances*, PhD thesis, Institute of Nuclear Physics, Krakow, 1986, DESY-F31-86-02.

[37] Particle Data Group, J. Beringer *et al.*, *Review of particle physics*, Phys. Rev. **D86** (2012) 010001, and 2013 partial update for the 2014 edition.

[38] M. Pivk and F. R. Le Diberder, *sPlot: a statistical tool to unfold data distributions*, Nucl. Instrum. Meth. **A555** (2005) 356, arXiv:physics/0402083.

[39] LHCb collaboration, R. Aaij *et al.*, *Prompt* K^0_S *production in* pp *collisions at* $\sqrt{s} = 0.9\,\mathrm{TeV}$, Phys. Lett. **B693** (2010) 69, arXiv:1008.3105.

[40] M. Ferro-Luzzi, *Proposal for an absolute luminosity determination in colliding beam experiments using vertex detection of beam-gas interactions*, Nucl. Instrum. Meth. **A553** (2005) 388.

[41] LHCb collaboration, R. Aaij *et al.*, *Absolute luminosity measurements with the LHCb detector at the LHC*, JINST **7** (2012) P01010, arXiv:1110.2866.

[42] P. Hopchev, *LHCb beam-gas imaging results*, arXiv:1107.1492.

[43] P. Hopchev, *Absolute luminosity measurement at LHCb*, PhD thesis, Université de Grenoble, Grenoble, 2011, CERN-THESIS-2011-210.

[44] C. Barschel, *Precision luminosity measurement at LHCb with beam-gas imaging*, PhD thesis, Fakultät für Mathematik, Informatik and Naturwissenschaften der RWTH Aachen University, Aachen, 2013.

[45] CMS collaboration, S. Chatrchyan *et al.*, *Measurement of the* $\Upsilon(1\mathrm{S})$, $\Upsilon(2\mathrm{S})$ *and* $\Upsilon(3\mathrm{S})$ *polarizations in* pp *collisions at* $\sqrt{s} = 7\,\mathrm{TeV}$, Phys. Rev. Lett. **110** (2013) 081802, arXiv:1209.2922.

[46] LHCb collaboration, R. Aaij *et al.*, *Measurement of* J/ψ *polarization in* pp *collisions at* $\sqrt{s} = 7\,\mathrm{TeV}$, Eur. Phys. J. **C73** (2013) 2631, arXiv:1307.6379.

[47] LHCb collaboration, R. Aaij *et al.*, *Measurement of* $\psi(2S)$ *polarisation in* pp *collisions at* $\sqrt{s} = 7\,\text{TeV}$, LHCb-PAPER-2013-067, in preparation.

[48] ALICE collaboration, B. Abelev *et al.*, J/ψ *polarization in* pp *collisions at* $\sqrt{s} = 7\,\text{TeV}$, Phys. Rev. Lett. **108** (2012) 082001, arXiv:1111.1630.

[49] R. Aaij *et al.*, *The LHCb trigger and its performance in 2011*, JINST **8** (2013) P04022, arXiv:1211.3055.

[50] CDF collaboration, D. Acosta *et al.*, Υ *production and polarization in* $p\overline{p}$ *collisions at* $\sqrt{s} = 1.8\,\text{TeV}$, Phys. Rev. Lett. **88** (2002) 161802.

[51] D0 collaboration, V. M. Abazov *et al.*, *Measurement of inclusive differential cross sections for* $\Upsilon(1S)$ *production in* $p\overline{p}$ *collisions at* $\sqrt{s} = 1.96\,\text{TeV}$, Phys. Rev. Lett. **94** (2005) 232001, arXiv:hep-ex/0502030.

[52] L. S. Kisslinger and D. Das, Υ *production in* pp *collisions for forward rapidities at LHC*, Mod. Phys. Lett. **A28** (2013) 1350067, arXiv:1207.3296.

[53] L. S. Kisslinger, M. X. Liu, and P. McGaughey, *Heavy quark qtate production in* pp *collisions*, Phys. Rev. **D84** (2011) 114020, arXiv:1108.4049.

[54] L. S. Kisslinger, Υ *production in* pp *collisions at LHC*, Mod. Phys. Lett. **A27** (2012) 1250074, arXiv:1201.1033.